**Cell Death and Differentiation (1998) 5,** 953–962

http://www.stockton-press.co.uk/cdd

# Apoptosis, in human monocytic THP.1 cells, results in the release of cytochrome c from mitochondria prior to their ultracondensation, formation of outer membrane discontinuities and reduction in inner membrane potential

**Jianguo Zhuang[1], David Dinsdale[1] and Gerald M. Cohen[1,2]**

[1] MRC Toxicology Unit, University of Leicester, Hodgkin Building, P O Box 138, Lancaster Road, Leicester, LEI 9HN, UK.
[2] corresponding author: MRC Toxicology Unit, University of Leicester, Hodgkin Building, P O Box 138, Lancaster Road, Leicester, LEI 9HN, UK.
tel: + 44 (0)116 252 5589; fax: + 44 (0)116 252 5616;
email: gmc2@le.ac.uk

Received 31.3.98; revised 25.6.98; accepted 6.7.98
Edited by P. Nicotera

## Abstract

**Induction of apoptosis in human monocytic THP.1 cells by etoposide or N-tosyl-L-phenylalanyl chloromethyl ketone resulted in release of mitochondrial cytochrome c, formation of ultracondensed mitochondria, development of outer mitochondrial membrane discontinuities and a reduction in mitochondrial membrane potential ($\Delta\Psi_m$), as well as externalisation of phosphatidylserine, caspase-3 and -7 activation, proteolysis of poly(ADP-ribose) polymerase and lamin B1. The caspase inhibitor, benzyloxycarbonyl-Val-Ala-Asp (OMe) fluoromethyl ketone inhibited all these ultrastructural and biochemical characteristics of apoptosis except for the release of cytochrome c. Release of mitochondrial cytochrome c was a late event in non-apoptotic cell death occurring after commitment to cell death and without caspase activation. Thus apoptosis is characterised by release of mitochondrial cytochrome c prior to formation of ultracondensed mitochondria and a reduction in $\Delta\Psi_m$ and by a mechanism independent of rupture of the outer mitochondrial membrane.**

**Keywords:** cytochrome c; apoptosis; mitochondrial ultracondensation; mitochondrial discontinuities; caspases

**Abbreviations:** $DiOC_6(3)$, 3,3′ dihexyloxacarbocyanine iodide; $\Delta\Psi_m$, mitochondrial membrane potential; PARP, poly(ADP-ribose)polymerase; TPCK, N-tosyl-L-phenylalanyl chloromethyl ketone; PS, phosphatidylserine; Z-VAD.fmk, Benzyloxycarbonyl-Val-Ala-Asp (OMe) fluoromethyl ketone.

## Introduction

Apoptosis is a fundamental form of cell death which plays a major role in the development and homeostasis of multicellular organisms (Arends and Wyllie, 1991). Disturbances in apoptosis are important in cancer, acquired immunodeficiency syndrome and some neurodegenerative disorders (Thompson, 1995). Apoptotic cell death comprises an initial commitment phase followed by an execution phase, which is characterised by a consistent series of distinct morphological changes (Earnshaw, 1995), suggesting the existence of a common execution machinery. Many of the characteristic morphological and biochemical changes of apoptosis result from the cleavage of cellular proteins, such as poly (ADP-ribose) polymerase (PARP) and lamins (Kaufmann *et al*, 1993) by a family of caspases (formerly known as interleukin-1$\beta$ converting enzyme-like proteases) (Alnemri *et al*, 1996). Caspases exist in cells as inactive proenzymes and are cleaved at specific aspartate residues, generating a large and small subunit, which together form the active enzyme (Thornberry and Molineaux, 1995; Kumar and Lavin, 1996; Cohen, 1997). The precise substrate specificity of most caspases is unknown but PARP is cleaved by caspases-3 and -7 (Lazebnik *et al*, 1994; Fernandes-Alnemri *et al*, 1995), whereas lamins are preferentially cleaved by caspase-6 (Orth *et al*, 1996; Takahashi *et al*, 1996). Apoptosis can be modulated by a wide variety of agents (Steller, 1995; Wyllie, 1995), including irreversible cell permeable caspase inhibitors, such as benzyloxycarbonyl-Val-Ala-Asp (OMe) fluoromethyl ketone (Z-VAD.fmk) (Cohen, 1997) and the cation $Zn^{2+}$ (Fraker and Telford, 1997). $Zn^{2+}$ inhibits apoptosis possibly by inhibiting a $Ca^{2+}/Mg^{2+}$-dependent endonuclease and/or the caspases (Cohen and Duke, 1984; Perry *et al*, 1997; Wolf *et al*, 1997).

Recently much attention has been paid to the role of mitochondria in cell death. Release of mitochondrial cytochrome c or reduction in mitochondrial membrane potential ($\Delta\Psi_m$) is an early feature of many models of apoptosis (Liu *et al*, 1996; Petit *et al*, 1996; Zamzami *et al*, 1995). Cytochrome c together with ATP/dATP and Apaf-1 results in the activation of caspase-9, which in turn activates other caspases, such as caspase-3 (Liu *et al*, 1996; Li *et al*, 1997; Zou *et al*, 1997). Although the mechanism of cytochrome c release from the mitochondrial intermembrane space is not known, three hypotheses have been proposed (Reed, 1997). First, opening of the mitochondrial permeability transition pore or 'megachannel' results in a reduction of $\Delta\Psi_m$ and osmotic swelling, with subsequent rupture of the outer membrane and release of cytochrome c (Petit *et al*, 1996). Second, the presence of a specific channel for cytochrome c in the outer membrane, with Bax being a possible candidate (Reed, 1997). Third, mitochondrial swelling and rupture of the outer membrane result in release of cytochrome c but without loss of $\Delta\Psi_m$ (Vander Heiden *et al*, 1997).

We now demonstrate that, in apoptotic THP.1 cells, the release of mitochondrial cytochrome c precedes the reduction in $\Delta\Psi_m$, ultracondensation of the mitochondria and rupture of the outer mitochondrial membrane. These results support the hypothesis that this release occurs through a channel and results in activation of caspases which in turn leads to further mitochondrial changes. In marked contrast, release of cytochrome c is a late event in non-apoptotic cell death.

## Results

### Inhibition of PS externalisation and proteolysis of PARP and lamin B1 by Z-VAD.fmk and $Zn^{2+}$

Incubation of THP.1 cells for 4 h with either etoposide (25 $\mu$M), a DNA topoisomerase II inhibitor, or TPCK (75 $\mu$M), a chymotrypsin-like serine protease inhibitor, resulted in the induction of apoptosis, assessed by the externalisation of PS (Figure 1A). $Zn^{2+}$ caused a concentration-dependent inhibition of the induction of apoptosis by both etoposide and TPCK (Figure 1A) but alone it did not induce PS externalisation (data not shown). Z-VAD.fmk (50 $\mu$M), a cell membrane permeable caspase inhibitor, also inhibited etoposide- or TPCK-induced apoptosis (Figure 1A). Control cells contained only intact PARP (116 kD) and lamin B1 ($\sim$67 kD) (Figure 1B and C, lane 1). Induction of apoptosis by either etoposide or TPCK was accompanied by the cleavage of PARP to its characteristic signature 85 kD fragment (Figure 1B lanes 2 and 7) and of lamin B1 to its $\sim$46 kD fragment (Figure 1C lanes 2 and 7). This cleavage of PARP and lamin B1 was completely blocked by Z-VAD.fmk (Figure 1B and C lanes 6 and 11), consistent with earlier observations (MacFarlane *et al*, 1997; Zhu *et al*, 1997). In cells treated with either etoposide or TPCK, $Zn^{2+}$ caused a concentration-dependent inhibition of the cleavage of both PARP and lamin B1 (Figure 1B and C, lanes 3–5 and 8–10), the latter being more susceptible to this inhibition. $Zn^{2+}$ (1 mM) clearly prevented the cleavage of PARP after etoposide treatment (Figure 1B lane 5) but did not completely block that after TPCK treatment (Figure 1B lane 10). These data are compatible with the cleavage of PARP and lamin B1 being mediated by distinct caspases and the potent inhibition of caspase-6 activity by $Zn^{2+}$ (Takahashi *et al*, 1996). Cleavage of lamin B1 and PARP suggested the activation of caspase-6 and of caspases-3 and/or -7 respectively (Fernandes-Alnemri *et al*, 1995; Orth *et al*, 1996; Takahashi *et al*, 1996). In order to investigate if $Zn^{2+}$ was affecting the processing of the caspases or inhibiting their activity, we examined its effects on the processing of caspases-3 and -7.

### Z-VAD.fmk and $Zn^{2+}$ inhibit the processing of caspases-3 and -7

Untreated control cells showed the presence of the intact $\sim$32 kD proform of caspase-3 (Figure 1D lane 1) and $\sim$35 kD proform of caspase-7 (Figure 1E lane 1). Processing of caspase-3 at Asp 175 between the large and small subunits yields a p20 subunit, which is further processed at Asp 9 and Asp 28 to yield p19 and p17 subunits (Fernandes-Alnemri *et al*, 1996), whereas processing of caspase-7 occurs at Asp198 between the large and small subunits, followed by cleavage at Asp 23 to yield the p19 large subunit (Fernandes-Alnemri *et al*, 1995). Induction of apoptosis with either etoposide or TPCK was accompanied by a reduction in the proforms of caspases-3 and -7 together with the formation of their respective catalytically-active large subunits (Figure 1D and E, lanes 2 and 7). Cleavage of caspases-3 and -7 was more extensive with TPCK treatment than with etoposide, commensurate with the greater induction of apoptosis by this stimulus (Figure 1A). $Zn^{2+}$ caused a concentration dependent inhibition of the processing of both caspase-3 and caspase-7 (Figure 1D and E, lanes 3–5 and 8–10). $Zn^{2+}$ (0.5–1 mM) completely inhibited the processing of caspase-3 in etoposide-treated cells (Figure 1D lanes 4 and 5), and largely but not completely inhibited that observed in TPCK-

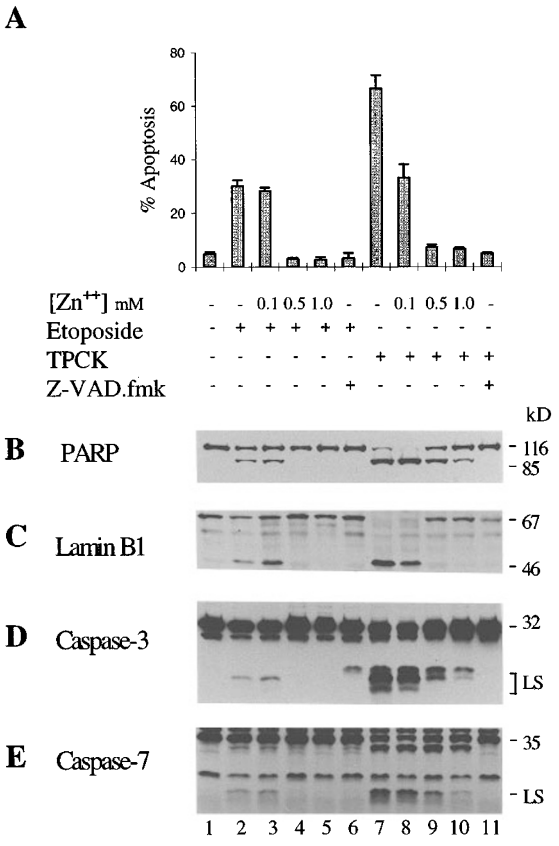


**Figure 1** Z-VAD.fmk and $Zn^{2+}$ inhibit PS exposure, cleavage of PARP and lamin B 1 and processing of caspases-3 and -7. THP.1 cells were incubated for 4 h either alone (lane1), with etoposide (25 $\mu$M) (lanes 2–6) or TPCK (75 $\mu$M) (lanes 7–11) in the presence of Z-VAD.fmk (50 $\mu$M) (lanes 6 and 11) or $Zn^{2+}$ (0.1–1 mM) (lanes 3–5 and 8–10) as indicated. (**A**) The induction of apoptosis was assessed by externalisation of PS by flow cytometry as described in Materials and Methods. Results were expressed as mean $\pm$S.E.M of at least three experiments. Cells were analyzed by Western blot analysis using antibodies to (**B**) PARP and (**C**) lamin B1. Cells were also analyzed for the cleavage of the (**D**) 32-kD pro-caspase-3 and (**E**) 35-kD pro-caspase-7 to their catalytically active large subunits (LS)

treated cells (Figure 1D lanes 9 and 10). Similarly $Zn^{2+}$ (1 mM) completely inhibited the processing of caspase-7 to its catalytically active p 19 large subunit following treatment with etoposide (Figure 1E, lane 5) and largely inhibited formation of the p 19 subunit induced by TPCK (Figure 1E, lane 10). This residual amount of processed caspase-3 and/or caspase-7 was most likely responsible for the small amount of PARP cleavage observed in these cells (Figure 1B lane 10). $Zn^{2+}$ alone did not induce the processing of either caspase-3 or -7 (data not shown). Z-VAD.fmk clearly blocked the processing of caspases-3 and -7 (Figure 1D and Figure E, lanes 6 and 11). However a small amount of a slightly larger immunoreactive fragment ($\sim$p20) of caspase-3 was observed in etoposide co-treated cells (Figure 1D lane 6). The lack of PARP cleavage (Figure 1B lane 6) indicated that this fragment was catalytically inactive. Thus both $Zn^{2+}$ and Z-VAD.fmk inhibit apoptosis by inhibiting either the processing of the effector caspases, -3 and -7 or a stage(s) upstream of this processing.

## Release of mitochondrial cytochrome c occurs upstream of the reduction in mitochondrial membrane potential ($\Delta\Psi_m$) during apoptosis

Recent studies have implied a key role for the release of mitochondrial cytochrome c in apoptosis. We wished to investigate the importance of this release in the induction of apoptosis in THP.1 cells, its relationship to $\Delta\Psi_m$ and its susceptibility to $Zn^{2+}$ or Z-VAD.fmk. Incubation with etoposide resulted in a time-dependent increase in both apoptosis, as assessed by PS exposure, and in the number of cells with decreased $\Delta\Psi_m$ (Figure 2A). This treatment also resulted in a time-dependent cytosolic accumulation of cytochrome c (Figure 2B lanes 2–6). Significant changes in all these parameters were clearly observed after 2 h treatment. Z-VAD.fmk and $Zn^{2+}$ inhibited the etoposide-induced reduction in $\Delta\Psi_m$, whereas alone these agents did not affect $\Delta\Psi_m$ (Table 1). Although $Zn^{2+}$ and Z-VAD.fmk both clearly inhibited the fall in $\Delta\Psi_m$, their effects on cytochrome c release were clearly different (Figure 2B). $Zn^{2+}$ (1.0 mM) but not Z-VAD.fmk blocked the etoposide-induced cytosolic accumulation of cytochrome c (Figure 2B lanes 7 and 8). The absence of cytochrome oxidase (subunit II) in the cytosolic extracts confirmed that the samples were free from mitochondrial contamination (Figure 2B). Thus Z-VAD.fmk prevented all the biochemical changes of apoptosis including the processing of caspases-3 and -7, the cleavage of PARP and lamins and the fall in $\Delta\Psi_m$ except for the release of mitochondrial cytochrome c. These data suggest that the release of cytochrome c is an independent event which occurs upstream of the fall in $\Delta\Psi_m$ and prior to caspase activation. Further support for this conclusion was provided by the data with TPCK, which caused a time-dependent increase in the percentage of cells with a reduced $\Delta\Psi_m$ (Figure 2C lanes 2–6). This increase was prevented by both $Zn^{2+}$ and Z-VAD.fmk (Figure 2C lanes 7 and 8). TPCK also induced a time-dependent release of mitochondrial cytochrome c (Figure 2C lanes 2–6), which was not blocked by either $Zn^{2+}$ or Z-VAD.fmk (Figure 2C lanes 7 and 8). These data show that $Zn^{2+}$ inhibited an etoposide- but not a TPCK-induced signal upstream of the release of cytochrome c. In TPCK-induced apoptosis the release of cytochrome c was already evident at 1 h, earlier than either

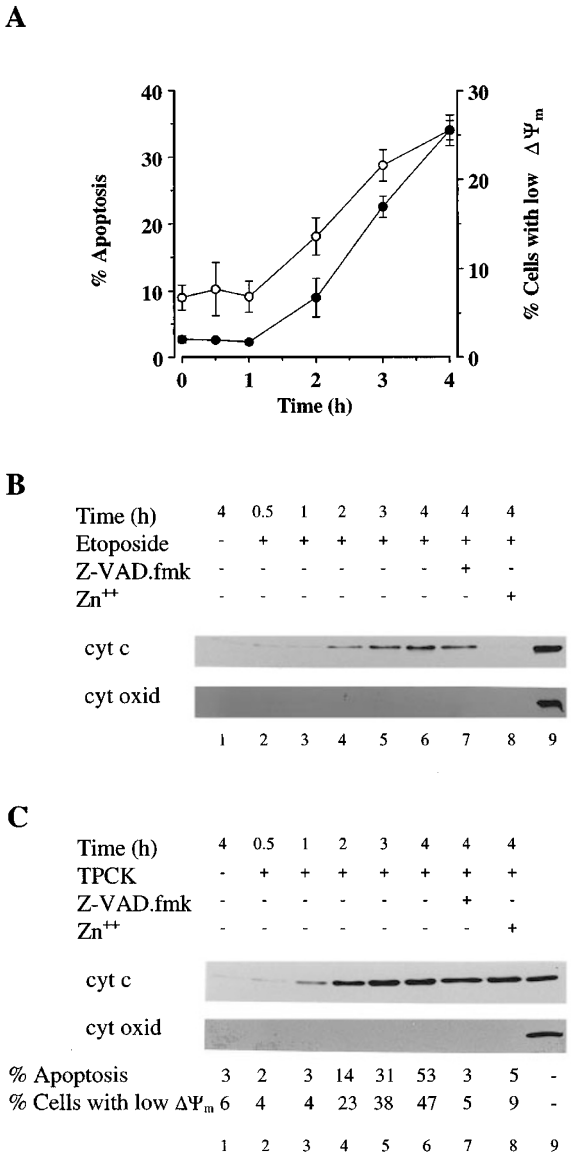


**Figure 2** Cytochrome c release is upstream of the decrease in $\Delta\Psi_m$. (**A**) Time course of induction of apoptosis by etoposide (25 $\mu$M) was determined by externalization of PS ●—● and the increase in the percentage of cells with decreased mitochondrial membrane potential ($\Delta\Psi_m$ )(o-o). Results were expressed as mean $\pm$ S.E.M. of at least three experiments. (**B**) Cells were incubated for the indicated times with etoposide (25 $\mu$M) either alone (lanes 2–6) or in the presence of Z-VAD.fmk (50 $\mu$M) (lane 7) or $Zn^{2+}$(1 mM) (lane 8). Cytosolic extracts were prepared and assessed by Western blot analysis for cytochrome c (cyt c) and also for cytochrome oxidase subunit II (cyt oxid), as a marker of mitochondrial contamination of the cytosolic extracts. Purified bovine heart cytochrome c (5 ng) (lane 9, upper blot) and 5 $\mu$l of the mitochondrial fraction following removal of the cytosolic extracts were loaded (lane 9, lower blot) as positive controls. (**C**) The time course of induction of apoptosis by TPCK (75 $\mu$M) either alone (lanes 2–6) or in the presence of Z-VAD.fmk (50 $\mu$M) (lane 7) or $Zn^{2+}$(1 mM) (lane 8) as determined by externalization of PS (% apoptosis) and by the % of cells with decreased $\Delta\Psi_m$. Cytosolic extracts were analyzed for cytochrome c and cytochrome oxidase II as described above

the externalisation of PS or the reduction in $\Delta\Psi_m$ (Figure 2C lane 3). At 1 h, caspase-3 was also processed to its catalytically-active large subunit, whereas cleavage of PARP was first observed at 2 h (data not shown). While these data did not distinguish whether cytochrome c release preceded processing of caspase-3 activation, results with both apoptotic stimuli demonstrated that the release of cytochrome c occurred upstream of the reduction in $\Delta\Psi_m$, during the induction of apoptosis.

## Mitochondrial ultracondensation and outer mitochondrial membrane discontinuities in apoptotic cells are inhibited by Z-VAD.fmk and $Zn^{2+}$

Unlike controls (Figure 3a), THP.1 cells incubated with etoposide developed many characteristic ultrastructural features of apoptosis, including condensation of chromatin into crescentic accumulations against the inner membrane of the nuclear envelope and an increase in cytoplasmic density. These changes were first observed at 3 h and were more pronounced at 4 h (Figure 3b). Cells treated with TPCK exhibited similar cytoplasmic changes but with less clumping and condensation of the heterochromatin (Zhu *et al*, 1997). Particularly striking was the presence of many ultracondensed mitochondria in both etoposide- and TPCK-treated cells (Figure 3b–d). A few of these organelles were observed as early as 2 h but were more prevalent by 4 h. We have defined these mitochondria as ultracondensed, based on their marked increase in matrix density and slight dilation of the outer compartment/intracristal space despite a marked reduction in volume. The reduced volume was inferred from their mean diameter ($262 \pm 58$ nm), in sections, compared with that of controls ($474 \pm 109$ nm). Similar ultracondensed mitochondria have been observed in tumour necrosis factor-induced apoptosis of a lymphoblastic cell line (Jia *et al*, 1997). These changes are distinct from the commonly described condensed mitochondria, which exhibit increased matrix density without any overall reduction in volume and correspond to state three respiration (Hackenbrock, 1968; Laiho and Trump, 1975). Ultracondensed mitochondria were invariably present in cells showing the nuclear and cytoplasmic changes but they were also found in some cells showing no other morphological signs of apoptosis (Figure 3b). While most mitochondria in the apoptotic cells were affected, some remained normal and a few showed condensation of only part of their inner compartment (Figure 3c and d). Discontinuities were observed in the outer membrane profile of many of the ultracondensed mitochondria and, although some could be attributed to obliquity of the section, many indicated exposure of inner-membrane-limited regions of the condensed matrix to the cytosol (Figure 3c and d). The contorted shapes of these organelles, together with the electron density of the surrounding cytoplasm in apoptotic cells militated against the clear identification of discontinuities in ultrathin sections. True discontinuities were, however, recognised by tilting these sections during examination. Further evidence was obtained from 0.5–1.0 $\mu$m sections contrasted *en bloc* and examined using an integrated energy filter to remove inelastically scattered electrons from the image. Z-VAD.fmk and $Zn^{2+}$ inhibited all the ultrastructural changes induced by etoposide and TPCK, including the mitochondrial and nuclear condensation together with the development of outer mitochondrial membrane discontinuities (Figure 4a and b and data not shown). These results demonstrate that the formation of both ultracondensed mitochondria and discontinuities in the outer mitochondrial membrane occurred downstream of the activation of caspases.

**Table 1** $Zn^{2+}$ and Z-VAD.fmk inhibit the decrease of $\Delta\Psi_m$ during etoposide-induced apoptosis

| Treatment | $Zn^{2+}$ (mM) | % cells with $\Delta\Psi_m$ |
|---|---|---|
| Control | – | $6.1 \pm 0.8$ |
| Etoposide | – | $24.4 \pm 1.2$ |
| Etoposide | 0.1 | $23.4 \pm 2.5$ |
| Etoposide | 0.5 | $11.4 \pm 4.7$ |
| Etoposide | 1.0 | $7.1 \pm 1.8$ |
| Etoposide+Z-VAD.fmk | | $3.9 \pm 0.7$ |
| $Zn^{2+}$ | 0.1 | $6.4 \pm 1.7$ |
| $Zn^{2+}$ | 0.5 | $5.9 \pm 1.2$ |
| $ZN^{2+}$ | 1.0 | $8.2 \pm 2.7$ |
| Z-VAD.fmk | | 2.6* |
| m-ClCCP | | $79.8 \pm 2.9$ |

THP.1 cells were incubated with etoposide (25 $\mu$M) for 4 h either alone or in the presence of the indicated concentrations of $Zn^{2+}$ or Z-VAD.fmk (50 $\mu$M) and the percentage of cells with decreased mitochondrial membrane potential ($\Delta\Psi_m$) was determined by flow cytometry. Cells were also incubated with the mitochondrial uncoupler, carbonyl cyanide m-chlorophenyl hydrazone (m-ClCCP, 50 $\mu$M) as a positive control. The results are expressed as the mean $\pm$ S.E.M. of at least three separate experiments except for *, which was the average of two experiments

## Cytochrome c release is a late event in non-apoptotic cell death

As $Zn^{2+}$ inhibits dexamethasone-induced internucleosomal cleavage of DNA but not apoptosis in thymocytes (Cohen *et al*, 1992), we investigated whether $Zn^{2+}$ prevented or merely delayed apoptosis. No processing of caspase-7 or cleavage of PARP was detected even after 24 h coincubation of THP.1 cells with etoposide and $Zn^{2+}$ (1 mM, data not shown). Nevertheless at 24 h, most of these cells were non-viable consistent with a non-apoptotic cell death. This non-apoptotic cell death was directly attributable to $Zn^{2+}$ rather than etoposide as $Zn^{2+}$ alone resulted in a similar time-dependent cytotoxicity (Figure 5A). Thus $Zn^{2+}$, at concentrations which inhibited drug-induced apoptosis during a 4 h incubation, resulted in a delayed cytotoxicity. The mechanism of this non-apoptotic cell death was investigated by monitoring both ATP levels and ultrastructural changes. $Zn^{2+}$ induced a time-dependent loss of intracellular ATP, which preceded a similar reduction in cell viability (Figure 5A). Ultrastructural studies revealed no signs of injury at 4 h (data not shown) whereas at 8 h cells were swollen. This was accompanied by a reduction in the density of the cytoplasm together with slight swelling of the lysosomes, endoplasmic reticulum and nuclei (Figure 4c). A few of these cells showed the development of flocculent densities within their mitochondria (Figure 4c). At 12 h these changes were more widespread and accompanied by chromatolysis or the clumping of heterochromatin into complex, densely-staining structures which were generally

isolated from the inner membrane of the nuclear envelope (Figure 4d). By 24 h most cells were clearly in the late stages of necrosis exhibiting flocculent densities in the mitochondrial matrix, chromatolysis and lysis of many organelles (data not shown). Thus the necrotic cells observed 24 h after treatment with $Zn^{2+}$ have died by oncosis, a process distinct from apoptosis (Majno and Joris, 1995). Oncosis is characterised by a loss of cellular ATP and cellular swelling leading to the

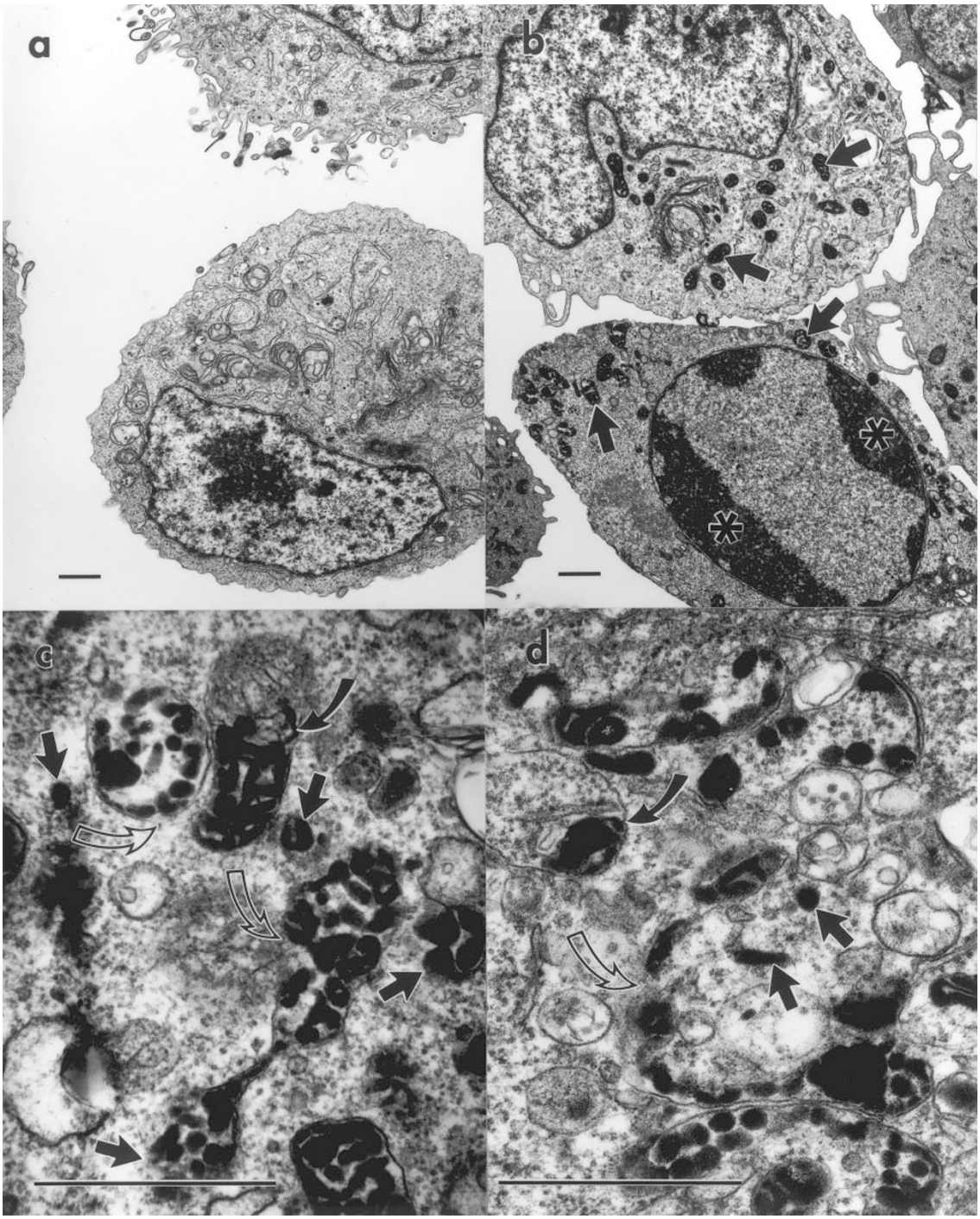


**Figure 3** Apoptotic stimuli induce mitochondrial ultracondensation and discontinuities in THP.1 cells. (**a**) Control THP.1 cells following incubation for 4 h in control medium showed normal ultrastructure. (**b**) Cells incubated with etoposide (25 $\mu$M) show many ultracondensed mitochondria (solid arrows) in a cell with normal chromatin distribution and in one with perinuclear accumulations of condensed chromatin (*). (**c**) The increase in matrix density was usually uniform but, in some mitochondria, only restricted regions were affected (solid curved arrow). (**d**) Similar changes were observed after treatment with TPCK (75 $\mu$M). Apparent discontinuities in the outer membrane of many of these mitochondria could be attributed to obliquity of the section (open curved arrows) but several of these organelles also showed disruption of this membrane resulting in the exposure of membrane-limited regions of the condensed matrix to the cytosol (solid arrows) (all bars =1 $\mu$m)

formation of necrotic cells. In order to determine at what stage these cells were irreversibly committed to die, cells were incubated with $Zn^{2+}$ for short periods of time and then transferred to a $Zn^{2+}$-free medium. At 24 h no loss of viability was observed when $Zn^{2+}$ was removed after 2 h incubation, whereas 50% of cells died when $Zn^{2+}$ was removed after 4 h

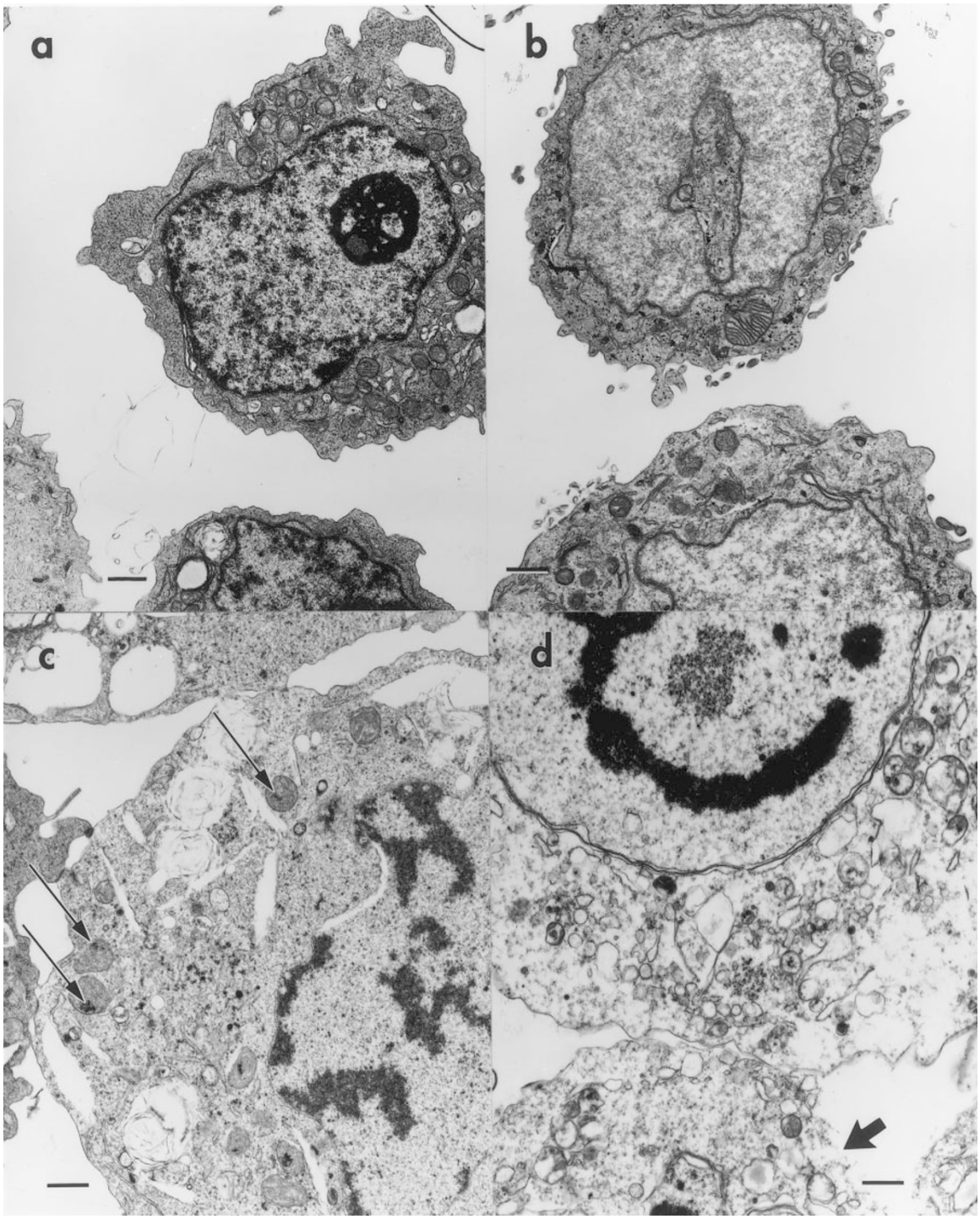


**Figure 4** Z-VAD.fmk and $Zn^{2+}$ inhibit the formation of mitochondrial ultracondensation and discontinuities. (**a**) Co-incubation of THP.1 cells with etoposide (25 $\mu$M) in the presence of $Zn^{2+}$ (0.5 mM) for 4 h resulted in complete inhibition of the formation of mitochondrial ultracondensation and discontinuities as well as other characteristic ultrastructural features of apoptosis. (**b**) Co-incubation of THP.1 cells with etoposide (25 $\mu$M) in the presence of Z-VAD.fmk (50 $\mu$M) for 4 h also prevented the formation of mitochondrial discontinuities and all the ultrastructural features of apoptosis. (**c**) Incubation with $Zn^{2+}$ (1 mM) for 8 h, resulted in a slight reduction in cytoplasmic density, swelling of lysosomes, endoplasmic reticulum and nuclei together with the clumping of heterochromatin and the development of flocculent densities within mitochondria (fine arrows). (**d**) Incubation with $Zn^{2+}$ (1 mM) for 12 h, resulted in a marked increase in the density of the clumped chromatin, reduction in cytoplasmic density, discontinuities in the cell membrane (solid arrow) and lysis of many of the organelles, including mitochondria. (all bars =1 $\mu$m)

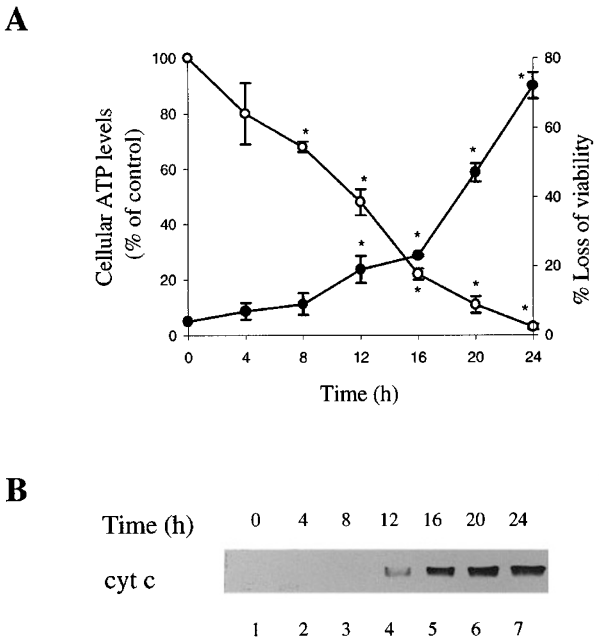


**Figure 5** Cytochrome c release is a late event during necrosis. THP.1 cells were incubated for up to 24 h in the presence of $Zn^{2+}$ (1 mM). (**A**) relative ATP levels (o-o) were measured as described in Materials and Methods. The level of ATP in the control cells at zero time was $9.0 \pm 0.6$ nmoles / $10^6$ cells. The percent loss of viability (●—●) was measured by uptake of propidium iodide by flow cytometry. Results are expressed as the mean ± S.E.M. of at least three experiments. The data were analyzed by Student's t test and differences between control and treatment of $P < 0.05$ were considered significant (*). **(B)** Cytosolic extracts were prepared at the indicated time points and assessed for cytochrome c (cyt c) by Western blot analysis. No detectable cytochrome oxidase subunit II, a marker of mitochondrial contamination, was detected in these samples (data not shown)

incubation. Thus cells were irreversibly committed to die as early as 4 h after exposure to $Zn^{2+}$, prior to the development of detectable ultrastructural changes.

While many recent studies have concentrated on a possible role of cytochrome c release in apoptosis, few if any have investigated a possible relationship between this release and other forms of cell death. $Zn^{2+}$ alone induced a time dependent increase in cytochrome c release, which was first observed at 12 h (Figure 5B), after the loss of intracellular ATP (Figure 5A) and ultrastructural changes which were observed at 8 h (Figure 4c). Thus release of mitochondrial cytochrome c is a late event in oncosis and does not play a significant role in this non-apoptotic form of cell death.

## Discussion

We have demonstrated that both $Zn^{2+}$ and Z-VAD.fmk inhibit apoptosis in human monocytic THP.1 cells, either by blocking the processing of both caspases-3 and -7 or by inhibiting a stage upstream of this processing. These results are consistent with recent studies showing that Z-VAD.fmk inhibits both the processing of caspases and their proteolytic activities (Armstrong *et al*, 1996; Jacobson *et al*, 1996; MacFarlane *et al*, 1997; Slee *et al*, 1996; Zhu *et al*, 1997) and that $Zn^{2+}$ is a general inhibitor of caspases (Perry *et al*, 1997; Stennicke and Salvesen, 1997; Wolf *et al*, 1997). Z-VAD.fmk completely inhibited the extensive processing of caspase-3 induced by TPCK but was less effective at inhibiting the more modest processing induced by etoposide (Figure 1D lanes 2, 6, 7 and 11), suggesting that the target of Z-VAD.fmk may be different in etoposide and TPCK-induced apoptosis.

### Release of cytochrome c is upstream of the reduction in $\Delta\Psi_m$

Release of mitochondrial cytochrome c together with caspase-9, Apaf-1 and ATP/dATP, forms a complex which then activates 'effector' caspases such as caspase-3 (Liu *et al*, 1996; Li *et al*, 1997. Several recent studies have also highlighted a role for a decrease in $\Delta\Psi_m$ as a key committed step in the induction of apoptosis (Petit *et al*, 1996; Zamzami *et al*, 1995). In our studies, both etoposide and TPCK caused a decrease in $\Delta\Psi_m$ and an increase in cytosolic cytochrome c (Table 1 and Figure 2). This increase corresponded with a reduction in the cytochrome c content of the mitochondrial fraction, as assessed by Western blot analysis (data not shown). It is not known whether all mitochondria within each cell are affected to a similar extent. However, the reduction in $\Delta\Psi_m$ was totally prevented by Z-VAD.fmk ( Table 1 and Figure 2C), indicating that this reduction is related to the development of apoptosis. The observation that pre-treatment with Z-VAD.fmk abolished the decrease in $\Delta\Psi_m$ without affecting the release of cytochrome c (Table 1 and Figure 2) suggests that the release of cytochrome c occurs upstream of the reduction in $\Delta\Psi_m$ or is an independent event, a result consistent with other studies (Kluck *et al*, 1997; Yang *et al*, 1997; Bossy-Wetzel *et al*, 1998). Further support for this hypothesis was provided by the finding that TPCK-induced cytochrome c release was clearly observed at 1 h, prior to the reduction in $\Delta\Psi_m$ or the increase in PS exposure (Figure 2C).

### Release of mitochondrial cytochrome c is upstream of the formation of ultracondensed mitochondria and discontinuities in the outer mitochondrial membrane

The transition of mitochondria from an orthodox to a condensed conformation is associated with a change from a resting (state 4) to an active (state 3) respiration (Hackenbrock, 1968; Lehninger, 1975). The characteristic increase in matrix density in the condensed conformation results from a reduction in the volume of the inner mitochondrial compartment, which is accompanied by a compensatory increase in the outer compartment/intracristal space resulting in little or no reduction in total volume of the organelle (Hackenbrock, 1968). The ultracondensed mitochondria described in the present study are distinct from the well-described condensed mitochondrial conformation and are characterised by a particularly pronounced increase in matrix density together with a marked decrease in overall volume (Figure 3b–d). The ultracondensed mitochondria in THP.1 cells exhibit similar features to those observed in apoptotic lymphoblastic leukaemic cells

(Jia *et al*, 1997), the 'pleomorphic micromitochondriosis' in apoptotic nodal myocytes (James *et al*, 1993) and the 'mitochondrial pyknosis' and 'hypercondensation' observed during apoptosis in a colon carcinoma cell line (Mancini *et al*, 1997). These changes were associated with an increased mitochondrial mass but with a decreased $\Delta\Psi_m$ (Mancini *et al*, 1997). Despite minor differences in the morphology of these examples of highly condensed mitochondria, they all share a pronounced increase in matrix density together with a marked reduction in the area of their profiles in thin sections. Mitochondria resembling the classical condensed form have been described as ultracondensed in some instances of cell death (Papadimitriou *et al*, 1994). In some systems, there appears to be a progression from the condensed to the ultracondensed form followed by deletion of the organelle (Jia *et al*, 1997; Mancini *et al*, 1997). In the present study co-incubation with Z-VAD.fmk resulted in mitochondria of normal appearance, with complete inhibition of the formation of ultracondensed mitochondria (Figure 4b) without affecting the release of mitochondrial cytochrome c (Figure 2B). Thus formation of ultracondensed mitochondria occurred downstream of caspase activation.

In apoptotic THP.1 cells, many ultracondensed mitochondria showed rupture of the outer membrane (Figure 3c and d) exposing regions of the condensed matrix to the cytosol. Mitochondria are susceptible to morphological change during delayed or inappropriate processing but control samples were devoid of any such condensation or discontinuities. Breaks in the outer mitochondrial membrane occur in the swollen mitochondria of apoptotic Jurkat and FL5.12 cells resulting in the redistribution of cytochrome c to the cytosol followed by a decrease of $\Delta\Psi_m$ (Vander Heiden *et al*, 1997). These changes are prevented by expression of Bcl-$x_L$ suggesting that it increases cell survival by modulating electrical and osmotic changes of mitochondria (Vander Heiden *et al*, 1997). In contrast the present study shows ultracondensation rather than swelling of mitochondria, in THP.1 cells, before the development of any other morphological features of apoptosis. As Z-VAD.fmk inhibited the formation of outer mitochondrial membrane discontinuities (Figure 4b), these changes were downstream of caspase activation. Thus our data have excluded two of the major hypotheses currently proposed for the release of mitochondrial cytochrome c, i.e. formation of outer mitochondrial membrane discontinuities and/ or resulting from a decrease in $\Delta\Psi_m$. An alternative mechanism for this release may be via a specific outer mitochondrial membrane channel. Bax, a proapoptotic member of the Bcl-2 family, forms channels in lipid membranes (Antonsson *et al*, 1997; Schlesinger *et al*, 1997) and has been proposed as a possible candidate for such a channel (Reed, 1997). Our data support the hypothesis that an initial mitochondrial perturbation results in the release of cytochrome c, which in the presence of Apaf-1 leads to activation of caspases-9 and -3. The activated caspases then cleave cellular proteins resulting in mitochondrial damage leading to mitochondrial ultracondensation and outer membrane discontinuities.

### Release of mitochondrial cytochrome c is a late event in non-apoptotic cell death

$Zn^{2+}$ alone induced a non-apoptotic cell death, consistent with the process of cell death normally referred to as oncosis (Majno and Joris, 1995; Trump *et al*, 1997). Irreversible commitment of these cells to die occurred at 4 h, prior to the release of cytochrome c. Thus this release is a late event in the oncotic death of THP.1 cells. The characteristic depletion of ATP in oncotic cells may preclude the activation of caspases, whereas in apoptotic cells, early release of mitochondrial cytochrome c following interaction with Apaf-1 and ATP/dATP results in the activation of caspases, so precipitating the biochemical and morphological features of apoptosis.

In summary we have demonstrated that during apoptosis release of mitochondrial cytochrome c occurs prior to ultracondensation of mitochondria and the reduction in $\Delta\Psi_m$, and by a mechanism independent of rupture of the outer mitochondrial membrane. These results provide indirect support for this release being mediated through a specific channel in the outer mitochondrial membrane.

## Materials and Methods

### Materials and chemicals

Media and serum were purchased from Gibco (Paisley, Scotland). All chemicals were obtained from Sigma Chemical Company (Poole, England) except for N-tosyl-L-phenylalanyl chloromethyl ketone (TPCK, Boehringer-Mannheim UK, Lewes, England), Z-VAD.fmk (Enzyme Systems Inc., Dublin, CA, USA) and 'AnalaR' zinc acetate dihydrate (BDH/Merck Ltd, Poole, England).

### Cell culture and treatment

THP.1 cells were maintained in RPMI 1640 supplemented with 10% heat-inactivated FBS and 2 mM glutamine in an atmosphere of 5% $CO_2$ in air at 37°C (Zhu *et al*, 1995). Logarithmically growing cells were used for all experiments. To induce apoptosis, $0.5 \times 10^6$ cells per ml were incubated in the presence of etoposide (25 $\mu$M) or TPCK (75 $\mu$M) as previously described (Zhu *et al*, 1995,1997). To assess the effects of Z-VAD.fmk (50 $\mu$M) and $Zn^{2+}$ (0.1 – 1.0 mM) on apoptosis, THP.1 cells were treated with these agents five minutes before exposure to the apoptotic stimulus.

### Flow cytometric analysis of phosphatidylserine (PS) exposure, cell viability, and mitochondrial membrane potential

Cells with externalised PS residues were detected by a FITC-labelled Annexin V binding assay (Martin *et al*, 1995). Briefly, $0.5 \times 10^6$ cells were pelleted and resuspended in 1 ml HEPES-buffered saline and incubated with 2.5$\mu$l FITC- labelled Annexin V (Bender MedSystems, Vienna, Austria) for 8 min at room temperature in the dark. After incubation, 2.5 $\mu$g propidium iodide was added and the sample was analysed in a Becton Dickinson FACScan flow cytometer. Cells, which included propidium iodide, were considered non-viable, expressed as a fraction (%) of the total cell population and gated-out. The percentage of the remaining, viable cells which were labelled with FITC was then determined. To measure mitochondrial membrane

potential ($\Delta\Psi_m$), $0.5 \times 10^6$ cells were incubated for 20 min at 37°C with the cationic lipophilic fluorochrome, 3,3′dihexyloxacarbocyanine iodide ($DiOC_6(3)$, 50 nM) (Molecular Probes Inc., Eugene, OR, USA), which is retained in mitochondria with a normal membrane potential (Petit *et al*, 1990). Control experiments were performed by incubating cells for a further 10 min at 37°C with carbonyl cyanide m-chlorophenyl hydrazone (m-ClCCP, 50 $\mu$M, Sigma), an uncoupling agent which abolishes the $\Delta\Psi_m$. Samples were immediately analysed by flow cytometry.

### Western blot analysis

Samples of $0.2 \times 10^6$ cells were prepared as described by MacFarlane *et al*, (1997). Cellular proteins were resolved on 15% (caspases-3 and -7) or 10% (PARP and lamin B1) SDS polyacrylamide gels and blotted onto nitrocellulose membranes (Hybond-C, Amersham, Little Chalfont, England). Intact PARP (116 kD) and its 85 kD signature fragment were detected with a mouse monoclonal antibody (C-210) (a gift from Dr. G. Poirier, Laval University, Quebec, Canada). Lamin B1 and its proteolytically derived fragment were probed with a mouse monoclonal antibody (Serotec Ltd., Oxford, England) as described (Zhu *et al*, 1997). Procaspase-3 and its catalytically active large subunit were detected with a rabbit polyclonal antibody raised against the p17 subunit of caspase-3 (a gift from Dr. D. Nicholson, Merck Frosst, Quebec, Canada) as described by MacFarlane *et al* (1997). Procaspase-7 and its catalytically active large subunit were detected with a rabbit polyclonal antibody raised against the large subunit of caspase-7 (MacFarlane *et al*, 1997). Final detection was achieved using the appropriate secondary antibody (goat anti-mouse IgG or goat anti-rabbit IgG) conjugated with HRP together with an enhanced chemiluminescence kit (Amersham, UK).

### Preparation of cytosolic extracts and assessment of cytochrome c

Isolation of the cytosolic extracts was essentially as described by Kluck *et al* (1997). Briefly, $50 \times 10^6$ THP.1 cells were washed twice in ice-cold PBS and resuspended in 200 $\mu$l of extraction buffer (220 mM mannitol, 68 mM sucrose, 50 mM PIPES/KOH, pH 7.5, 50 mM KCl, 5 mM EGTA, 2 mM $MgCl_2$, 1 mM dithiothreitol, 1 mM phenylmethylsulfonyl fluoride, 10 $\mu$g/ml leupeptin, 10 $\mu$g/ml pepstatin A and 10 $\mu$g/ml aprotinin). After 30 min incubation on ice, cells were homogenised using a glass Dounce homogeniser, with 40 strokes of the 'B' pestle. The homogenates were then centrifuged at 14 000 g, for 15 min at 4°C, and the resulting supernatants were used as the cytosolic extracts. Cytosolic protein (30 $\mu$g) was separated by SDS–PAGE, transferred to nitrocellulose membranes, and probed with a mouse monoclonal antibody recognising human cytochrome c (7H8.2C12) (PharMingen, San Diego, CA, USA) at a dilution of 1 : 1000. Final detection was as described above. Parallel samples, containing an equal amount of cytosolic protein, were checked by immunoblotting for mitochondrial contamination using the 12C4-F12 mouse monoclonal antibody (Molecular Probes) to mitochondrial membrane-bound cytochrome c oxidase (subunit II) as described by Kluck *et al* (1997).

### Electron microscopy

THP.1 cells ($3 \times 10^6$) were harvested as a pellet and processed as previously described (Cohen *et al*, 1992; Zhu *et al*, 1997). Duplicate samples were fixed with 2% glutaraldehyde in 0.1 M sodium cacodylate buffer (pH 7.4) at 4°C overnight and postfixed with 1% osmium tetroxide/1% potassium ferrocynanide overnight at 4°C. After fixation, cells were stained *en bloc* with 5% aqueous uranyl acetate overnight at room temperature, dehydrated, and embedded in Agar 100 epoxy resin. Sections, up to 1 $\mu$m were examined unstained by electron spectroscopic imaging using a Zeiss 902A electron microscope. Ultrathin sections were stained with lead citrate and examined in a Jeol 100-CXII electron microscope equipped with a rotating stage/eucentric goniometer.

### ATP measurements

Intracellular ATP was determined luminometrically using a bioluminescent somatic cell assay kit (Sigma) according to the manufacturer's instructions. The amount of light emitted was measured on a Wallac 1450 Microbeta Liquid Scintillation Counter (Wallac OY, Turku, Finland).

## References

Alnemri ES, Livingston DJ, Nicholson DW, Salvesen G, Thornberry NA, Wong WW and Yuan J (1996) Human ICE/CED-3 protease nomenclature. Cell 87: 171

Antonsson B, Conti F, Ciavatta A-M, Montessuit S, Lewis S, Martinou I, Bernasconi L, Bernard A, Mermod J-J, Mazzei G, Maundrell K, Gambale F, Sadoul R and Martinou J-C (1997) Inhibition of Bax channel-forming activity by Bcl-2. Science 277: 370–372

Arends MJ and Wyllie AH (1991) Apoptosis: mechanisms and roles in pathology. Int. Rev. Exp. Path. 32: 223–254

Armstrong RC, Aja T, Xiang J, Gaur S, Krebs JF, Hoang K, Bai X, Korsmeyer SJ, Karanewsky DS, Fritz LC and Tomaselli KJ (1996) Fas-induced activation of the cell death-related protease CPP32 is inhibited by Bcl-2 and by ICE family protease inhibitors. J. Biol. Chem. 271: 16850–16855

Bossy-Wetzel E, Newmeyer DD and Green DR (1998) Mitochondrial cytochrome c release in apoptosis occurs upstream of DEVD-specific caspase activation and independently of mitochondrial transmembrane depolarization. EMBO J. 17: 37–49

Cohen GM (1997) Caspases: the executioners of apoptosis. Biochem. J. 326: 1–16

Cohen GM, Sun X-M, Snowden RT, Dinsdale D and Skilleter DN (1992) Key morphological features of apoptosis may occur in the absence of internucleosomal DNA fragmentation. Biochem. J. 286: 331–334

Cohen JJ and Duke RC (1984) Glucocorticoid activation of a calcium-dependent endonuclease in thymocyte nuclei leads to cell death. J. Immunol. 132: 38–42

Earnshaw WC (1995) Nuclear changes in apoptosis. Curr. Opin. Cell. Biol. 7: 337–343

Fernandes-Alnemri T, Takahashi A, Armstrong R, Krebs J, Fritz L, Tomaselli KJ Wang L, Yu Z, Croce CM, Salveson G, Earnshaw WC, Litwack G and Alnemri ES (1995) Mch3, a novel human apoptotic cysteine protease highly related to CPP32. Cancer Res. 55: 6045–6052

Fernandes-Alnemri T, Armstrong RC, Krebs J, Srinivasula SM, Wang L, Bullrich F, Fritz LC, Trapani JA, Tomaselli KJ, Litwack G, Alnemri ES (1996) In vitro activation of CPP32 and Mch3 by Mch4, a novel human apoptotic cysteine protease containing two FADD-like domains. Proc. Natl. Acad. Sci. 93: 7464–7469

Fraker PJ and Telford WG (1997) A reappraisal of the role of zinc in life and death decisions of cells. Proc. Soc. Exp. Biol. Med. 215: 229–236

Hackenbrock CR (1968) Ultrastructural bases for metabolically linked mechanical activity in mitochondria. J. Cell. Biol. 37: 345–369

Jacobson MD, Weil M and Raff MC (1996) Role of CED-3/ICE-family proteases in staurosporine-induced programmed cell death. J. Cell. Biol. 133: 1041–1051

James TN, Terasaki F, Pavlovich ER and Vikhert AM (1993) Apoptosis and pleomorphic micromitochondriosis in the sinus nodes surgically excised from five patients with the long QT syndrome. J. Lab. Clin. Med. 122: 309–323

Jia L, Dourmashkin RR, Newland AC and Kelsey SM (1997) Mitochondrial ultracondensation, but not swelling, is involved in TNF$\alpha$-induced apoptosis in human T-lymphoblastic leukaemic cells. Leukemia Res. 21: 973–983

Kaufmann SH, Desnoyer S, Ottaviano Y, Davidson NE and Poirier GG (1993) Specific proteolytic cleavage of poly(ADP-ribose) polymerase: an early marker of chemotherapy-induced apoptosis. Cancer Res. 53: 3976–3985

Kluck RM, Bossy-Wetzel E, Green DR and Newmeyer DD (1997) The release of cytochrome c from mitochondria: a primary site for Bcl-2 regulation of apoptosis. Science 275: 1132 – 1136

Kumar S and Lavin MF (1996) The ICE family of cysteine proteases as effectors of cell death. Cell Death Differ. 3: 255 – 267

Laiho KU and Trump BF (1975) Studies on the pathogenesis of cell injury. Effects of inhibitors of metabolism and membrane function on the mitochondria of Ehrlich ascites tumor cells. Lab. Invest. 32: 163 – 182

Lazebnik YA, Kaufmann SH, Desnoyers S, Poirier GG and Earnshaw WC (1994) Cleavage of poly(ADP-ribose) polymerase by a proteinase with properties like ICE. Nature 371: 346 – 347

Lehninger AL (1975) Biochemistry. The Molecular Basis of Cell Structure and Function. 2nd ed. (New York: Worth Publishers) 1104 pp.

Li P, Nijhawan D, Budihardjo I, Srinivasula SM, Ahmad M, Alnemri ES and Wang X (1997) Cytochrome c and dATP-dependent formation of Apaf-1/caspase-9 complex initiates an apoptotic protease cascade. Cell 91: 479 – 489

Liu X, Kim CN, Yang J, Jemmerson R and Wang X (1996) Induction of apoptotic program in cell-free extracts: Requirements for dATP and cytochrome c. Cell 86: 147 – 157

MacFarlane M, Cain K, Sun X-M, Alnemri ES and Cohen GM (1997) Processing/ activation of at least four interleukin-1 $\beta$ converting enzyme-like proteases occurs during the execution phase of apoptosis in human monocytic tumor cells. J. Cell. Biol. 137: 469 – 479

Majno G and Joris I (1995) Apoptosis, oncosis, and necrosis. An overview of cell death. Amer. J. Path. 146: 3 – 15

Mancini M, Anderson BO, Caldwell E, Sedghinasab M, Paty PB and Hockenbery DM (1997) Mitochondrial proliferation and paradoxical membrane depolarization during terminal differentiation and apoptosis in a human colon carcinoma cell line. J. Cell. Biol. 138: 449 – 469

Martin SJ, Reutelingsperger CPM, McGahon AJ, Rader JA, van Schie RCAA, LaFace DM and Green DR (1995) Early redistribution of plasma membrane phosphatidylserine is a general feature of apoptosis regardless of the initiating stimulus: inhibition by overexpression of Bcl-2 and Abl. J. Exp. Med. 182: 1545 – 1556

Orth K, Chinnaiyan AM, Garg M, Froelich CJ and Dixit VM (1996) The CED-3/ICE like protease Mch-2 is activated during apoptosis and cleaves the death substrate lamin A. J. Biol. Chem. 271: 16443 – 16446

Papadimitriou JC, Drachenberg CB, Shin ML and Trump BF (1994) Ultrastructural studies of complement mediated cell death: a biological reaction model to plasma membrane injury. Virchows Archiv. 424: 677 – 685

Perry DK, Smyth MJ, Stennicke HR, Salvesen GS, Duriez P, Poirier GG and Hannun YA (1997) Zinc is a potent inhibitor of the apoptotic protease, caspase-3. J. Biol. Chem. 272: 18530 – 18533

Petit PX, O'Connor JE, Grunwald D and Brown SC (1990) Analysis of the membrane potential of rat- and mouse-liver mitochondria by flow cytometry and possible applications. Eur. J. Biochem. 194: 389 – 397

Petit PX, Susin S-A, Zamzami N, Mignotte B and Kroemer G (1996) Mitochondria and programmed cell death: back to the future. FEBS Letts. 396: 7 – 13

Reed JC (1997) Cytochrome c: can't live with it – can't live without it. Cell 91: 559 – 562

Schlesinger PH, Gross A, Yin X-M, Yamamoto K, Saito M, Waksman G and Korsmeyer SJ (1997) Comparison of the ion channel characteristics of proapoptotic BAX and antiapoptotic BCL-2. Proc. Natl. Acad. Sci. 94: 11357 – 11362

Slee EA, Zhu H, Chow SC, MacFarlane M, Nicholson DW and Cohen GM (1996) Benzyloxycarbonyl-Val-Ala-Asp (OMe) fluoromethylketone (Z-VAD.FMK) inhibits apoptosis by blocking the processing of CPP32. Biochem. J. 315: 21 – 24

Steller H (1995) Mechanisms and genes of cellular suicide. Science 267: 1445 – 1449

Stennicke HR and Salvesen GS (1997) Biochemical characteristics of caspases-3, -6, -7, and -8. J. Biol. Chem. 272: 25719 – 25723

Takahashi A, Alnemri ES, Lazebnik YA, Fernandes-Alnemri T, Litwack G, Moir RD, Goldman RD, Poirier GG, Kaufmann SH and Earnshaw WC (1996) Cleavage of lamin A by Mch2$\alpha$ but not CPP32: multiple interleukin 1$\beta$-converting enzyme-related proteases with distinct substrate recognition properties are active in apoptosis. Proc. Natl. Acad. Sci. 93: 8395 – 8400

Thompson CB (1995) Apoptosis in the pathogenesis and treatment of disease. Science 267: 1456 – 1462

Thornberry NA and Molineaux SM (1995) Interleukin-1$\beta$ converting enzyme: A novel cysteine protease required for IL-1$\beta$ production and implicated in programmed cell death. Protein Sci. 4: 3 – 12

Trump BF, Berezesky IK, Chang SH and Phelps PC (1997) The pathways of cell death: oncosis, apoptosis and necrosis. Toxicol Path. 25: 82 – 88

Vander Heiden MG, Chandel NS, Williamson EK, Schumacker PT and Thompson CB (1997) Bcl-$x_L$ regulates the membrane potential and volume homeostasis of mitochondria. Cell 91: 627 – 637

Wolf CM, Morana SJ and Eastman A (1997) Zinc inhibits apoptosis upstream of ICE/ CED-3 proteases rather than at the level of an endonuclease. Cell Death Differ 4: 125 – 129

Wyllie AH (1995) The genetic regulation of apoptosis. Curr. Opin. Genet. Dev. 5: 97 – 104

Yang J, Liu X, Bhalla K, Kim CN, Ibrado AM, Cai J, Peng TI, Jones DP and Wang X (1997) Prevention of apoptosis by Bcl-2: release of cytochrome c from mitochondria blocked. Science 275: 1129 – 1132

Zamzami N, Marchetti P, Castedo M, Zanin C, Vayssière JL, Petit PX and Kroemer G (1995). Reduction in mitochondrial potential constitutes an early irreversible step of programmed lymphocyte death in vivo. J. Exp. Med. 181: 1661 – 1672

Zhu H, Fearnhead HO and Cohen GM (1995) An ICE-like protease is a common mediator of apoptosis induced by diverse stimuli in human monocytic THP.1 cells. FEBS Letts. 374: 303 – 308

Zhu H, Dinsdale D, Alnemri ES and Cohen GM, (1997) Apoptosis in human monocytic THP.1 cells involves several distinct targets of N-tosyl-L-phenylalanyl chloromethyl ketone (TPCK). Cell Death Differ 4: 590 – 599

Zou H, Henzel WJ, Liu X, Lutschg A and Wang X (1997) Apaf-1, a human protein homologous to C. elegans CED-4, participates in cytochrome c-dependent activation of caspase-3. Cell 90: 405 – 413